AAC Journals.ASM.org

CYP2J2 and CYP2C19 Are the Major Enzymes Responsible for Metabolism of Albendazole and Fenbendazole in Human Liver Microsomes and Recombinant P450 Assay Systems

Zhexue Wu,[a] Doohyun Lee,[a] Jeongmin Joo,[a] Jung-Hoon Shin,[a] Wonku Kang,[b] Sangtaek Oh,[c] Do Yup Lee,[c] Su-Jun Lee,[d] Sung Su Yea,[d] Hye Suk Lee,[e] Taeho Lee,[a] Kwang-Hyeon Liu[a]

College of Pharmacy and Research Institute of Pharmaceutical Sciences, Kyungpook National University, Daegu, South Korea[a]; College of Pharmacy, Yeungnam University, Kyungpook, South Korea[b]; Department of Advanced Fermentation Fusion Science & Technology, Kookmin University, Seoul, South Korea[c]; College of Medicine, Inje University, Busan, South Korea[d]; College of Pharmacy and Integrated Research Institute of Pharmaceutical Sciences, The Catholic University of Korea, Bucheon, South Korea[e]

Albendazole and fenbendazole are broad-spectrum anthelmintics that undergo extensive metabolism to form hydroxyl and sulfoxide metabolites. Although CYP3A and flavin-containing monooxygenase have been implicated in sulfoxide metabolite formation, the enzymes responsible for hydroxyl metabolite formation have not been identified. In this study, we used human liver microsomes and recombinant cytochrome P450s (P450s) to characterize the enzymes involved in the formation of hydroxyalbendazole and hydroxyfenbendazole from albendazole and fenbendazole, respectively. Of the 10 recombinant P450s, CYP2J2 and/or CYP2C19 was the predominant enzyme catalyzing the hydroxylation of albendazole and fenbendazole. Albendazole hydroxylation to hydroxyalbendazole is primarily mediated by CYP2J2 (0.34 μl/min/pmol P450, which is a rate 3.9- and 8.1-fold higher than the rates for CYP2C19 and CYP2E1, respectively), whereas CYP2C19 and CYP2J2 contributed to the formation of hydroxyfenbendazole from fenbendazole (2.68 and 1.94 μl/min/pmol P450 for CYP2C19 and CYP2J2, respectively, which are rates 11.7- and 8.4-fold higher than the rate for CYP2D6). Correlation analysis between the known P450 enzyme activities and the rate of hydroxyalbendazole and hydroxyfenbendazole formation in samples from 14 human liver microsomes showed that albendazole hydroxylation correlates with CYP2J2 activity and fenbendazole hydroxylation correlates with CYP2C19 and CYP2J2 activities. These findings were supported by a P450 isoform-selective inhibition study in human liver microsomes. In conclusion, our data for the first time suggest that albendazole hydroxylation is primarily catalyzed by CYP2J2, whereas fenbendazole hydroxylation is preferentially catalyzed by CYP2C19 and CYP2J2. The present data will be useful in understanding the pharmacokinetics and drug interactions of albendazole and fenbendazole *in vivo*.

Albendazole and fenbendazole are benzimidazole compounds used as broad-spectrum anthelmintics against gastrointestinal nematodes and the larval stages of cestodes (1). Benzimidazole anthelmintics are extensively metabolized in domestic animals and humans. Animal and microsomal incubation studies have demonstrated rapid conversion of albendazole and fenbendazole to a sulfoxide metabolite and subsequently a sulfone metabolite (2–6). Sulfoxide metabolites are responsible for the systemic biological activity of benzimidazole drugs (7). Their metabolic patterns and the resultant pharmacokinetic behaviors are relevant in the attainment of high and sustained concentrations of pharmacologically active drugs/metabolites at the target parasite (8). Evidence from microsomal investigations in a number of species suggests that CYP3A4 and flavin-containing monooxygenase (FMO) are major enzymes responsible for the formation of sulfoxide metabolites from albendazole (4, 9, 10) and fenbendazole (4, 5) (Fig. 1). Recently, Lee et al. (11) reported that the rates of albendazole sulfoxide formation from albendazole by the recombinant CYP2J2 (rCYP2J2) isoform were significantly higher than those by the recombinant CYP3A4 (rCYP3A4) isoform, indicating the importance of the CYP2J2 isoform in albendazole sulfoxide formation (Fig. 1).

Hydroxy metabolite formation is one of the most common biotransformation pathways in drug metabolism. Fenbendazole is metabolized to hydroxyfenbendazole in rat liver microsomes (5). In cattle following intravenous administration, more than 50% of the dose was excreted as hydroxyfenbendazole in the feces (12). In addition, Lee et al. (11) also reported that hydroxyalbendazole was formed in the incubation mixtures of albendazole and the rCYP2J2 isoform. However, the involvement of the cytochrome P450 (P450) isoform in the metabolism of albendazole and fenbendazole is poorly understood.

The increased use of benzimidazole drugs against systemic infections, often for long periods and in combination with other agents, suggests that identifying the specific metabolites formed by individual P450s is essential for prediction of drug interactions and adverse events associated with therapy (9). For example, albendazole has been used for the treatment of the gastrointestinal helminthiases and also used to cure neurocysticercosis, which requires long medication periods of about 7 to 30 days (13). Although it exerts broad-spectrum coverage with high cure rates

Received 22 April 2013 Returned for modification 9 June 2013
Accepted 13 August 2013
Published ahead of print 19 August 2013
Address correspondence to Kwang-Hyeon Liu, dstlkh@knu.ac.kr, or Taeho Lee, tlee@knu.ac.kr.
Z.W. and D.L. contributed equally to this article.

doi:10.1128/AAC.00843-13

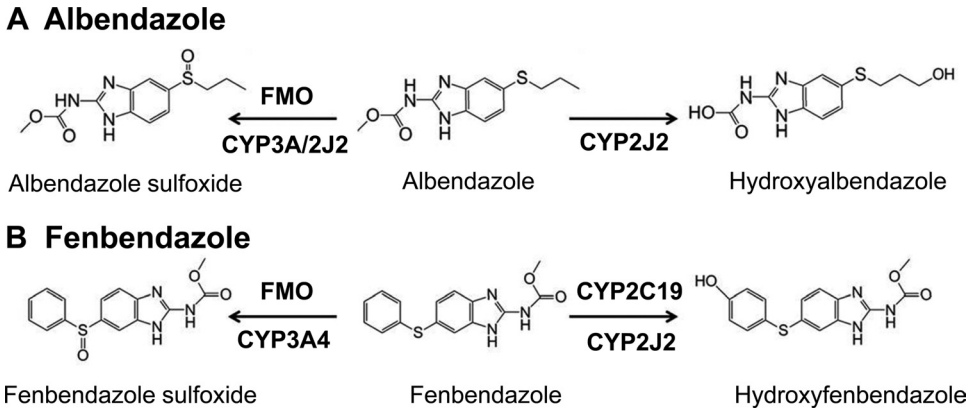

FIG 1 Proposed metabolic pathways of albendazole (A) and fenbendazole (B) in human liver microsomes.

against helminthic infections, multiple studies have indicated a lack of understanding of the causes of the large variations in the concentrations of the albendazole metabolite in human blood (14, 15) and possible adverse effects, such as infantile eczema, associated with albendazole treatment during pregnancy (16, 17). Investigation of the detailed metabolism of anthelminthic agents would be helpful for the assessment of the risks and benefits of routine treatment with these drugs. Therefore, the objective of this study was to identify and kinetically characterize the P450 isoforms responsible for the formation of the corresponding hydroxyl metabolites from albendazole and fenbendazole. The information from these studies will allow a better understanding of the factors affecting benzimidazole pharmacokinetics and drug interactions.

MATERIALS AND METHODS

Chemicals and reagents. Hydroxyebastine was obtained from Toronto Research Chemicals (North York, ON, Canada). Albendazole, astemizole, danazol, diethyldithiocarbamate, ebastine, fenbendazole, furafylline, ketoconazole, mebendazole, quercetin, quinidine, sulfaphenazole, tranylcypromine, ticlopidine, triethylenethiophophoramide (thio-TEPA), β-NADP (β-NADP$^+$), $MgCl_2$, potassium phosphate (KH_2PO_4), D-glucose-6-phosphate (G6P), and glucose-6-phosphate dehydrogenase (G6PDH) were purchased from Sigma-Aldrich (St. Louis, MO). Solvents were high-pressure liquid chromatography (HPLC) grade (Fisher Scientific Co., Pittsburgh, PA), and the other chemicals were of the highest quality available. Pooled human liver microsomes (H161), human liver microsomes (HLMs) from 14 different single donors, and 10 human recombinant P450 isoforms (1A2, 2A6, 2B6, 2C8, 2C9, 2C19, 2D6, 2E1, 2J2, and 3A4; Supersomes) were purchased from BD Biosciences (San Jose, CA). Human P450s 2A6, 2B6, 2C8, 2C9, 2C19, 2E1, 2J2, and 3A4 are coexpressed with human P450 reductase and cytochrome b_5; however, P450s 1A2 and 2D6 are coexpressed only with human P450 reductase. Information regarding protein content, P450 content, and enzymatic activity is supplied by the manufacturer (BD Biosciences).

Preparation of hydroxyalbendazole and hydroxyfenbendazole standards. Hydroxyalbendazole and hydroxyfenbendazole were synthesized by three-step reactions from 5-chloro-2-nitroaniline using 3-mercaptopropan-1-ol and 4-mercaptophenol, respectively (Fig. 2) (18–21).

(i) Procedure for synthesis of compounds A1 and B1. To a solution of 5-chloro-2-nitroaniline (523 mg, 3.00 mmol) in acetonitrile (15 ml) was added thiol [3-mercaptopropan-1-ol for 3-(3-amino-4-nitrophenylthio) propan-1-ol (compound A1) or 4-mercaptophenol for 4-(3-amino-4-nitrophenylthio)phenol (compound B1), 3.30 mmol] and K_2CO_3 (498 mg, 3.6 mmol) at room temperature. The reaction mixture was refluxed for 5 h. After cooling to room temperature, the K_2CO_3 was filtered off. The filtrate was concentrated *in vacuo*. The subsequent residue was purified by column chromatography to give compound A1 (96%) or B1 (97%). Compound A1: orange solid; ^{1}H nuclear magnetic resonance (NMR) (400 MHz, dimethyl sulfoxide [DMSO]-d_6) δ 7.86 (d, J = 9.1 Hz, 1H), 7.44 (s, 2H), 6.84 (d, J = 2.0 Hz, 1H), 6.49 (dd, J = 9.1, 2.1 Hz, 1H), 4.62 (t, J = 5.2 Hz, 1H), 3.54 to 3.49 (m, 2-H), 3.02 (t, J = 7.3 Hz, 2H), 1.85 to 1.73 (m, 2H). Compound B1: orange solid; ^{1}H NMR (400 MHz, DMSO-d_6) δ 10.05 (s, 1H), 7.85 (d, J = 9.1 Hz, 1H), 7.43 (s, 2H), 7.38 (d, J = 8.3 Hz, 2H), 6.90 (d, J = 8.2 Hz, 2H), 6.48 (d, J = 1.8 Hz, 1H), 6.26 (dd, J = 9.1, 2.0 Hz, 1H).

(ii) Procedure for synthesis of compounds A2 and B2. To a solution of a nitro compound [compound A1 for 3-(3,4-diaminophenylthio)propan-1-ol (compound A2) or compound B1 for 4-(3,4-diaminophenylthio) phenol (compound B2), 2.00 mmol] in ethanol (20 ml) was added tin(II)

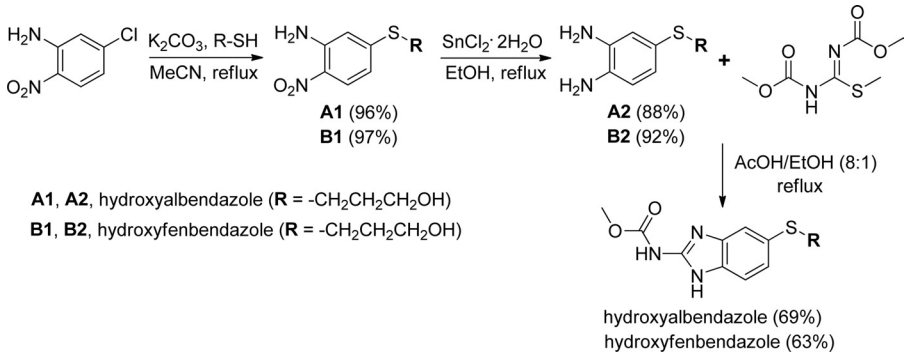

FIG 2 Synthesis of hydroxyalbendazole and hydroxyfenbendazole. MeCN, acetonitrile; EtOH, ethanol; AcOH, acetic acid.

chloride dehydrate (2.48 g, 11.0 mmol). The reaction mixture was refluxed for 12 h. After cooling to room temperature, the reaction mixture was basified to pH 9 using a 3 N sodium hydroxide solution. Ethyl acetate (50 ml) was added and then filtered through Celite, followed by washing with water and ethyl acetate. The aqueous layer was separated and then extracted twice with ethyl acetate. The combined organic layers were washed with brine, dried over $MgSO_4$, filtered, and concentrated *in vacuo* to give compound A2 (88%) or B2 (92%). Compound A2: yellow oil; ^{1}H NMR (400 MHz, DMSO-d_6) δ 6.59 (t, J = 1.1 Hz, 1H), 6.44 (d, J = 1.1 Hz, 2H), 4.53 (br s, 4H), 4.44 (t, J = 5.2 Hz, 1H), 3.46 to 3.41 (m, 2H), 2.70 (t, J = 7.3 Hz, 2H), 1.64 to 1.56 (m, 2H). Compound B2: brown solid; ^{1}H NMR (400 MHz, DMSO-d_6) δ 9.43 (s, 1H), 7.02 (d, J = 8.7 Hz, 2H), 6.68 (d, J = 8.7 Hz, 2H), 6.56 (dd, J = 1.6, 0.6 Hz, 1H), 6.49 to 6.43 (m, 2H), 4.64 (br s, 2H), 4.56 (br s, 2H).

(iii) Procedure for synthesis of hydroxyalbendazole and hydroxyfenbendazole. To a solution of diamino compound (compound A2 for hydroxyalbendazole or compound B2 for hydroxyfenbendazole, 1.00 mmol) in acetic acid-ethanol (8:1, 45 ml) was added 1,3-bis(methoxycarbonyl)-2-methyl-2-thiopseudourea (234 mg, 1.10 mmol) at room temperature. The reaction mixture was refluxed for 3 h. After cooling to room temperature, the reaction mixture was concentrated *in vacuo*. The subsequent residue was diluted with dichloromethane and washed with water. The organic layer was dried over $MgSO_4$ and evaporated under vacuum. The residue was purified by column chromatography to give the desired hydroxyalbendazole or hydroxyfenbendazole. Methyl-{5-[(3-hydroxypropyl)thio]-1*H*-benzo[*d*]imidazol-2-yl}carbamate (hydroxyalbendazole): white solid; ^{1}H NMR (400 MHz, DMSO-d_6) δ 11.60 (br s, 2H), 7.42 (d, J = 1.4 Hz, 1H), 7.34 (d, J = 8.2 Hz, 1H), 7.10 (dd, J = 8.2, 1.8 Hz, 1H), 4.49 (t, J = 5.2 Hz, 1H), 3.75 (s, 2H), 3.50 to 3.44 (m, 2H), 2.91 (t, J = 7.3 Hz, 2H), 1.73 to 1.60 (m, 1H); liquid chromatography (LC)-mass spectrometry (MS) (electrospray ionization [ESI]) m/z 282 ($[M + 1]^+$). Methyl-{5-[(4-hydroxyphenyl)thio]-1*H*-benzo[*d*]imidazol-2-yl} carbamate (hydroxyfenbendazole): white solid; ^{1}H NMR (400 MHz, DMSO-d_6) δ 11.61 (br s, 2H), 9.67 (s, 1H), 7.33 (d, J = 8.3 Hz, 1H), 7.28 (d, J = 1.5 Hz, 1H), 7.20 (d, J = 8.7 Hz, 2H), 7.01 (dd, J = 8.3, 1.8 Hz, 1H), 6.76 (d, J = 8.7 Hz, 2H), 3.74 (s, 3H); LC-MS (ESI) m/z 316 ($[M + H]^+$).

Metabolism of albendazole and fenbendazole in HLMs and with recombinant P450s. The optimal conditions for microsomal incubation for the formation of metabolites of albendazole and fenbendazole were determined in the linear range. In all experiments, albendazole and fenbendazole were dissolved and serially diluted to the required concentrations with methanol, and the final concentration of organic solvent did not exceed 1%.

The incubation mixture, containing either 5 μl of microsomes (5 mg of protein/ml of stock) or 5 μl of recombinant P450 (diluted to 50 pmol/ml with phosphate buffer, pH 7.4) and various concentrations of albendazole and fenbendazole (0 to 100 μM), was reconstituted in 100 mM phosphate buffer (pH 7.4) and preincubated for 5 min at 37°C. To initiate the reaction, an NADPH-generating system (including 3.3 mM G6P, 1.3 mM β-$NADP^+$, 3.3 mM $MgCl_2$, and 500 units/ml G6PDH) and the reaction mixtures (final volume, 100 μl) were incubated for 20 min at 37°C in a thermo-shaker (AllSheng, Hangzhou, China). The reaction was terminated by placing the incubation tubes on ice and by immediately adding 50 μl of acetonitrile. After adding the internal standard (IS; mebendazole, 1 μM), the incubation mixtures were centrifuged at 10,000 × *g* for 5 min at 4°C, and aliquots of the supernatant were injected into an LC-tandem MS (LC-MS/MS) system.

Chemical inhibition studies with HLMs. Pooled HLMs (H161) and a P450-selective inhibitor were added to an incubation mixture similar to that described above. The concentration of albendazole or fenbendazole was 5 μM. The P450 isoform-selective inhibitors used were furafylline (1 and 5 μM) for CYP1A2, tranylcypromine (1 and 5 μM) for CYP2A6, thio-TEPA (1 and 5 μM) for CYP2B6, quercetin (2 and 10 μM) for CYP2C8, sulfaphenazole (1 and 5 μM) for CYP2C9, ticlopidine (0.2 and 1 μM) for CYP2C19, quinidine (0.2 and 1 μM) for CYP2D6, diethyldithiocarbamate (5 and 25 μM) for CYP2E1, danazol (1 and 5 μM) for CYP2J2, and ketoconazole (0.2 and 1 μM) for CYP3A. In all of the experiments the inhibitors were dissolved and serially diluted to the required concentrations with methanol, and the final concentration of methanol did not exceed 1%. Except for the addition of P450 isoform-selective inhibitors, all other incubation conditions were similar to those described above. For the assays with mechanism-based inhibitors (furafylline and ticlopidine), the reaction mixture was preincubated for 15 min at 37°C in the presence of inhibitor and an NADPH-generating system before the addition of substrate (albendazole or fenbendazole). After adding the internal standard and centrifugation as described above, aliquots of the supernatant were analyzed on an LC-MS/MS system.

Correlation experiments. Albendazole (5 μM) or fenbendazole (5 μM) was incubated with HLMs from 14 different livers to examine the formation of hydroxyalbendazole and hydroxyfenbendazole from albendazole and fenbendazole, respectively, relative to specific P450 activity. The activity of each P450 isoform was determined using LC-MS/MS as previously described (22). Isoform-specific reaction markers were used to determine the activity of each P450: phenacetin *O*-deethylation with 50 μM phenacetin (CYP1A2), coumarin 7-hydroxylation with 5 μM coumarin (CYP2A6), bupropion hydroxylation with 50 μM bupropion (CYP2B6), paclitaxel 6′-hydroxylation with 10 μM paclitaxel (CYP2C8), tolbutamide 4-methylhydroxylation with 100 μM tolbutamide (CYP2C9), *S*-mephenytoin 4-hydroxylation with 100 μM *S*-mephenytoin (CYP2C19), dextromethorphan *O*-demethylation with 5 μM dextromethorphan (CYP2D6), chlorzoxazone 6-hydroxylation with 50 μM chlorzoxazone (CYP2E1), ebastine hydroxylation with 1 μM ebastine (CYP2J2), and midazolam 1′-hydroxylation with 5 μM midazolam (CYP3A). The correlation coefficients between the rates of hydroxyalbendazole or hydroxyfenbendazole formation from albendazole or fenbendazole, respectively, and the activity of each P450 isoform were calculated by parametric regression analysis (SAS version 8.01; SAS Institute, Cary, NC). A P value of ≤0.05 was considered to indicate statistical significance.

LC-MS/MS analysis of hydroxyalbendazole and hydroxyfenbendazole. The concentrations of hydroxyalbendazole and hydroxyfenbendazole in HLM cultures were quantified using LC-MS/MS as described elsewhere, with some modification (2, 11). The system consisted of a Thermo Vantage triple-quadrupole mass spectrometer (Thermo Fisher Scientific, San Jose, CA), coupled with a Thermo Accela HPLC system (Thermo Fisher Scientific). The compounds were separated on a reversed-phase column (Cosmosil C_{18}; 2.0 mm [inner diameter] by 75 mm; particle size, 2.5 μm; Nacalai Tesque, Inc., Kyoto, Japan) with an isocratic mobile phase consisting of acetonitrile and water (30/70, vol/vol) containing 0.1% formic acid. The mobile phase was eluted at a flow rate of 0.2 ml/min. For identification of hydroxyalbendazole and hydroxyfenbendazole, mass spectra were recorded by electrospray ionization in positive mode. The operating conditions were optimized by flow injection of an analyte and were as follows: capillary temperature, 350°C; vaporizer temperature, 300°C; sheath gas pressure, 35 arbitrary units; auxiliary gas, 10 arbitrary units; nitrogen gas flow rate, 8 liters/min; spray voltage, 4,000 V; collision energy, 20 eV. Quadrupoles Q1 and Q3 were set on unit resolution. Quantitation was performed by selective reaction monitoring (SRM) of the protonated precursor ion $[M + H]^+$ and the related product ion for hydroxyalbendazole and hydroxyfenbendazole using the internal standard (1 μM mebendazole) to establish peak area ratios. Ions was detected by monitoring the transitions of m/z 282 → 250 for hydroxyalbendazole, m/z 316 → 284 for hydroxyfenbendazole, and m/z 296 → 264 for mebendazole (IS). The analytical data were processed by Xcalibur (version 2.1) software. The lower limits of quantification for the two analytes were 1.0 nM. The interassay precision for the analyte was less than 15%.

Data analysis. Results are presented as the means ± standard deviations (SDs) of estimates obtained from three different liver microsome

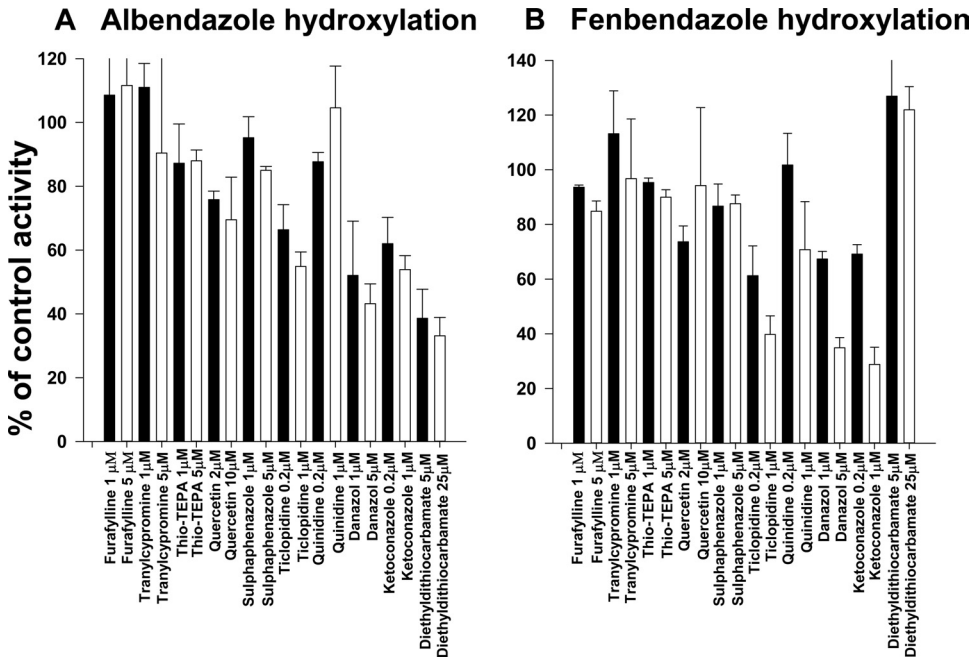

FIG 3 Effects of P450 isoform-specific inhibitors on the metabolism of albendazole (A) and fenbendazole (B) by human liver microsomes. Albendazole or fenbendazole (5 μM) was incubated with pooled human liver microsomes in the presence of various inhibitors. Error bars represent standard deviations ($n = 3$). The P450 isoform-selective inhibitors used were as follows: furafylline (1 and 5 μM) for CYP1A2, tranylcypromine (1 and 5 μM) for CYP2A6, thio-TEPA (1 and 5 μM) for CYP2B6, quercetin (2 and 10 μM) for CYP2C8, sulfaphenazole (1 and 5 μM) for CYP2C9, ticlopidine (0.2 and 1 μM) for CYP2C19, quinidine (0.2 and 1 μM) for CYP2D6, diethyldithiocarbamate (5 and 25 μM) for CYP2E1, danazol (1 and 5 μM) for CYP2J2, and ketoconazole (0.2 and 1 μM) for CYP3A.

preparations in triplicate experiments. The apparent kinetic parameters of hydroxyalbendazole and hydroxyfenbendazole metabolism were determined by fitting the unweighted kinetic data from HLMs and recombinant P450s to a one-enzyme Michaelis-Menten equation, a sigmoidal (Hill) equation model $\{V = V_{max} \times [S]^n/(K^n_m + [S]^n)\}$, and a substrate inhibition model $\{V = V_{max}/(1 + K_m/[S] + [S]/K_{si})\}$, where the calculated parameters were the maximum rate of metabolite formation (V_{max}), the Michaelis constant (K_m), intrinsic clearance (CL_{int}; which is equal to V_{max}/K_m), the Hill coefficient (n), and the substrate inhibition constant (K_{si}) and where [S] is the substrate concentration. Percent inhibition was calculated by the ratio of metabolite formation with and without the specific inhibitor. Calculations were performed using WinNonlin software (Pharsight, Mountain View, CA).

RESULTS AND DISCUSSION

In this study, we present a detailed characterization of the P450 isoforms responsible for the formation of hydroxyalbendazole and hydroxyfenbendazole from albendazole and fenbendazole, respectively, using human liver P450 enzymes (Fig. 1). These results demonstrate that albendazole is metabolized to hydroxyalbendazole mainly by CYP2J2 and fenbendazole is metabolized to hydroxyfenbendazole by CYP2C19 and CYP2J2. These data provide an important resource for accumulation of focused clinical information that will facilitate understanding of the pharmacokinetics, therapeutic efficacies, drug interactions, and safety profile of albendazole and fenbendazole.

We provide evidence that albendazole hydroxylation is catalyzed predominantly by CYP2J2. First, the rates of hydroxyalbendazole formation were reduced by 1 μM ticlopidine (~40%), 5 μM danazol (~60%), and 25 μM diethyldithiocarbamate (~65%), a selective CYP2C19 (23), a selective CYP2E1 (22), and a strong CYP2J2 (24) inhibitor, respectively (Fig. 3A). The selective CYP3A inhibitor (22) ketoconazole (1 μM) also inhibited (~45%) albendazole hydroxylation. This inhibition was due to nonselective inhibition of CYP2J2 activity by ketoconazole. To confirm these data, we evaluated inhibition of CYP2J2 activity by ketoconazole. Ketoconazole showed moderate inhibition of CYP2J2-mediated ebastine hydroxylation, with a 50% inhibitory concentration (IC_{50}) of 2.1 μM in HLMs (our unpublished data). Similar inhibition of CYP2J2 activity by ketoconazole was observed in the CYP2J2-mediated formation of metabolites of terfenadine and astemizole in HLMs (24). Second, recombinant CYP2J2 metabolized albendazole more efficiently than did other P450s, with few contributions from CYP2C19 and CYP2E1 (Fig. 4A). We noted that the contributions of the CYP2C19 and CYP2E1 isoforms to albendazole hydroxylation appeared to be minor, as the CL_{int}s for hydroxyalbendazole formation by CYP2C19 and CYP2E1 were 3.9- and 8.1-fold lower, respectively, than the CL_{int} for CYP2J2 (Table 1). Moreover, *S*-mephenytoin 4-hydroxylation (a marker of CYP2C19 activity) and chlorzoxazone 6-hydroxylation activity (a marker of CYP2E1 activity) in 14 individual HLMs exhibited no correlation with the rate of formation of hydroxyalbendazole from albendazole ($P > 0.05$) (Table 2). Third, the rates of hydroxyalbendazole formation from albendazole were significantly correlated ($P < 0.001$) with CYP2J2-mediated ebastine hydroxylation activity (a marker of CYP2J2 activity (25–27). The significant correlation between CYP3A activity and albendazole hydroxylation may not be associated with the actual involvement of CYP3A in albendazole hydroxylation. Instead, the correlation is likely derived from the significant corre-

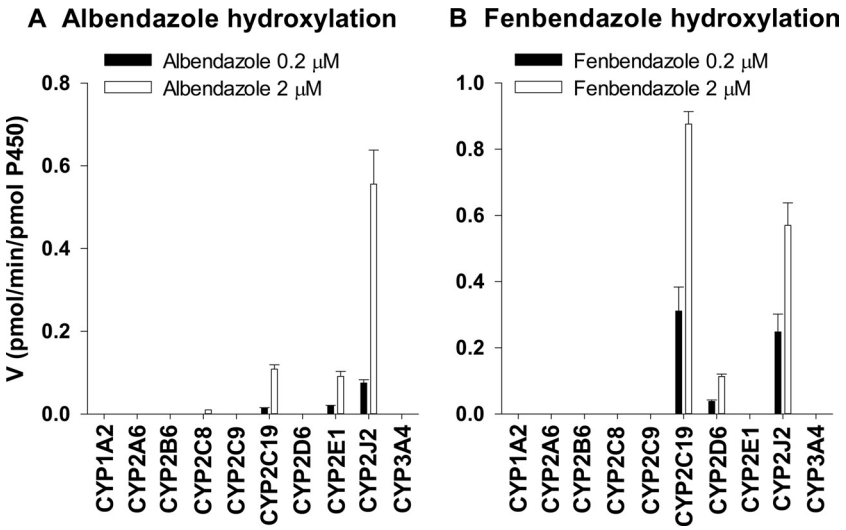

FIG 4 Representative plots of the formation of hydroxyl metabolites from albendazole (A) and fenbendazole (B) by cDNA-expressed human P450 isoforms. Human cDNA-expressed P450s 1A2, 2A6, 2B6, 2C8, 2C9, 2C19, 2D6, 2E1, 2J2, and 3A4 were incubated with albendazole or fenbendazole (0.2 and 2 μM). Error bars represent standard deviations ($n = 3$).

lation between the activity of CYP3A and CYP2J2 (Pearson $r = 0.60$; $P = 0.023$) in the bank of HLMs tested. Several studies have also reported cross correlations among P450 isoform activities (28–32).

The kinetics of formation of hydroxyalbendazole from albendazole by recombinant CYP2C19 (rCYP2C19) and rCYP2J2 were characterized by the Hill equation (Fig. 5A and C). The Eadie-Hofstee plots of hydroxyalbendazole formation revealed concave relationships (data not shown), indicating negative ($n = 0.56$ and 0.82 for CYP2C19 and CYP2J2, respectively) cooperativity (33). The rate of hydroxyalbendazole formation by recombinant CYP2E1 versus albendazole concentrations was characterized by an initial rapid increase at lower concentrations, followed by a progressive decline at higher substrate concentrations (Fig. 5B). Comparison of the goodness-of-fit values generated from these data indicates that a substrate inhibition equation enzyme model provided a better fit than did other models. The corresponding Eadie-Hofstee plot indicated a hook in the upper region (data are not shown), which is characteristic of substrate inhibition. Similar substrate inhibition profiles have previously been observed for CYP1A2-mediated KR-32570 *O*-demethylation (33), CYP2J2-mediated hydroxyebastine carboxylation (25), and CYP2E1-mediated *p*-nitrophenol oxidation (34), and such profiles are suggestive of multiple substrate-binding sites (or multiple regions within a single active site). Although this observation may have no clinical relevance because the expected concentrations of albendazole in human plasma after a person takes the usual dosage (400 mg, twice daily) (35) are much lower than the substrate inhibition constants ($K_{si} = 3.17$ μM) that we obtained here, it does offer insight into the characteristics of the enzyme. The kinetic parameters estimated from the recombinant P450 isoforms are shown in Table 1. The intrinsic clearance value (0.34 μl/min/pmol P450) of hydroxyalbendazole formation by CYP2J2 was markedly higher than the values for CYP2C19 (0.042 μl/min/pmol P450) and CYP2E1 (0.088 μl/min/pmol P450) (Table 1), indicating that CYP2J2 is the major metabolizing enzyme responsible for hydroxyalbendazole formation.

The specific hepatic P450 enzymes involved in the formation of hydroxyfenbendazole from fenbendazole have not been identified so far. Both ticlopidine and danazol markedly inhibited (>60%) hydroxyfenbendazole formation (Fig. 3B). The inhibition by ketoconazole, a CYP3A inhibitor, might be derived from its inhibi-

TABLE 1 Kinetics of hydroxyalbendazole and hydroxyfenbendazole formation from albendazole and fenbendazole, respectively, by cDNA-expressed P450 isoforms[b]

Substrate and P450	V_{max} (pmol/min/pmol P450)	K_m (μM)	n[a]	K_i (μM)	V_{max}/K_m (μl/min/pmol P450)
Albendazole					
CYP2C19	0.28	6.69	0.56		0.042
CYP2E1	0.25	2.83		3.17	0.088
CYP2J2	0.65	1.91	0.82		0.34
Fenbendazole					
CYP2C19	0.91	0.34		60.7	2.68
CYP2D6	0.13	0.57	0.78		0.23
CYP2J2	0.62	0.32		98.6	1.94

[a] n represents the Hill coefficient.
[b] The values are estimated from nonlinear least regression analysis using WinNonlin software ($n = 3$ experiments).

TABLE 2 Correlation between rates of hydroxyalbendazole and hydroxyfenbendazole formation from albendazole and fenbendazole, respectively, with P450 activities in 14 human liver microsome samples[a]

Activity	P450 isoform	*r* (*P* value[b])	
		Albendazole	Fenbendazole
Phenacetin *O*-deethylation	CYP1A2	0.24 (0.40)	0.41 (0.15)
Coumarin 7-hydroxylation	CYP2A6	0.09 (0.75)	0.09 (0.75)
Bupropion hydroxylation	CYP2B6	0.23 (0.41)	0.02 (0.93)
Paclitaxel 6α-hydroxylation	CYP2C8	0.49 (0.07)	0.50 (0.07)
Tolbutamide 4-methylhydroxylation	CYP2C9	0.44 (0.11)	0.39 (0.17)
S-Mephenytoin 4-hydroxylation	CYP2C19	0.30 (0.29)	0.78 (<0.01)
Dextromethorphan *O*-demethylation	CYP2D6	0.03 (0.90)	0.22 (0.45)
Chlorzoxazone 6-hydroxylation	CYP2E1	0.50 (0.07)	0.44 (0.11)
Ebastine hydroxylation	CYP2J2	0.91 (<0.01)	0.59 (<0.03)
Midazolam 1′-hydroxylation	CYP3A	0.60 (0.02)	0.63 (0.02)

[a] Albendazole and fenbendazole were used at 5 μM each. Data were analyzed using Pearson's parametric correlation test. The activity of each P450 isoform was determined using the respective specific substrate probe reaction, as described previously (22).
[b] A *P* value of <0.05 was considered to be statistically significant.

tory potential against CYP2J2 activity (IC_{50} = 2.1 μM). Human recombinant CYP2C19 and CYP2J2 formed hydroxyfenbendazole from fenbendazole (Fig. 4B). We also noted that the contribution of the CYP2D6 isoform to fenbendazole hydroxylation appeared to be minor, as the CL_{int} values for hydroxyfenbendazole formation by CYP2D6 were 11.7- and 8.4-fold lower than those for CYP2C19 and CYP2J2, respectively (Table 1), and the rate of dextromethorphan *O*-demethylation (a marker of CYP2D6 activity) in 14 individual HLMs exhibited no correlation with the rate of hydroxyfenbendazole formation from fenbendazole (*P* = 0.45)

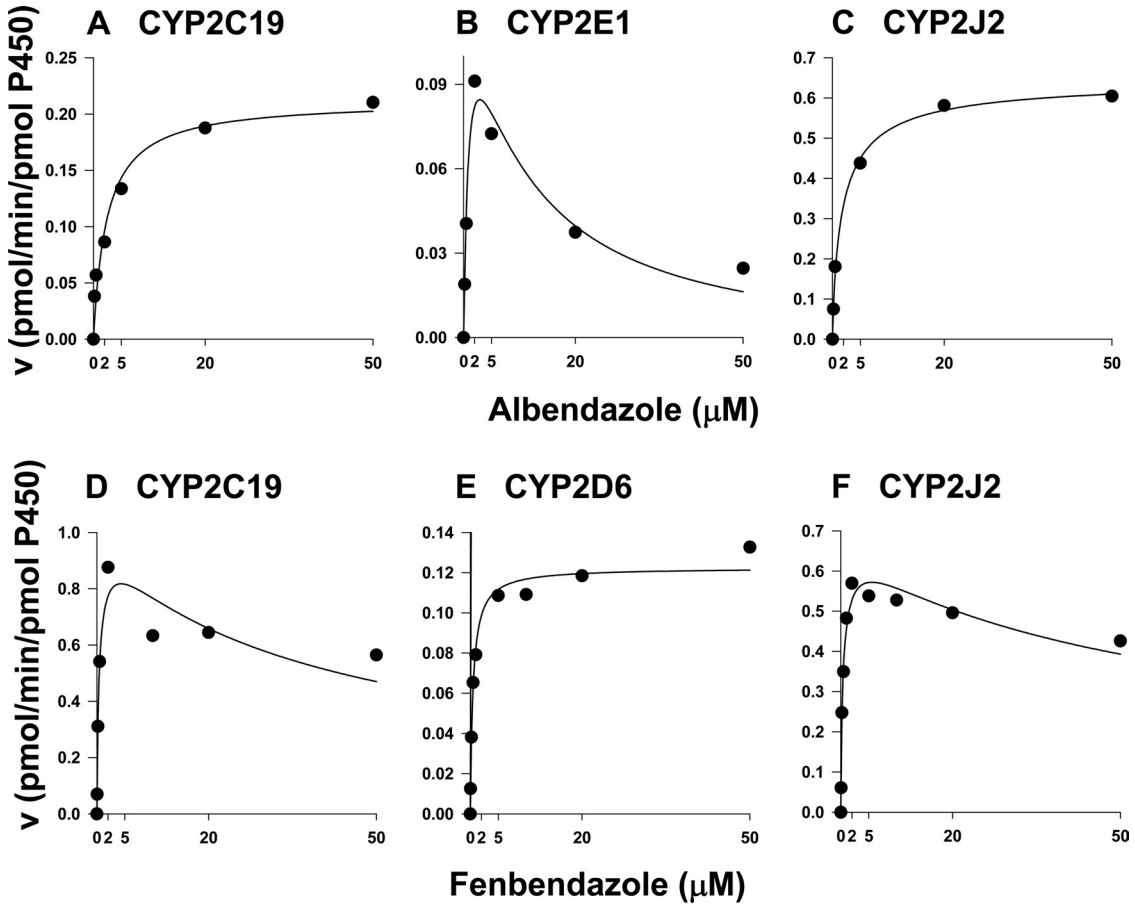

FIG 5 Kinetics for hydroxyalbendazole (A to C) or hydroxyfenbendazole (D to F) formation from albendazole or fenbendazole by recombinant human CYPC19, CYP2D6, CYP2E1, and/or CYP2J2. An increasing concentration of substrate (0 to 100 μM) was incubated with human cDNA-expressed P450s and an NADPH-generating system at 37°C for 20 min. The velocity (pmol/min/pmol P450) versus the albendazole or fenbendazole concentration was fit to a Hill or substrate inhibition equation (see "Data analysis" in Materials and Methods). Each data point represents the mean of triplicate incubations.

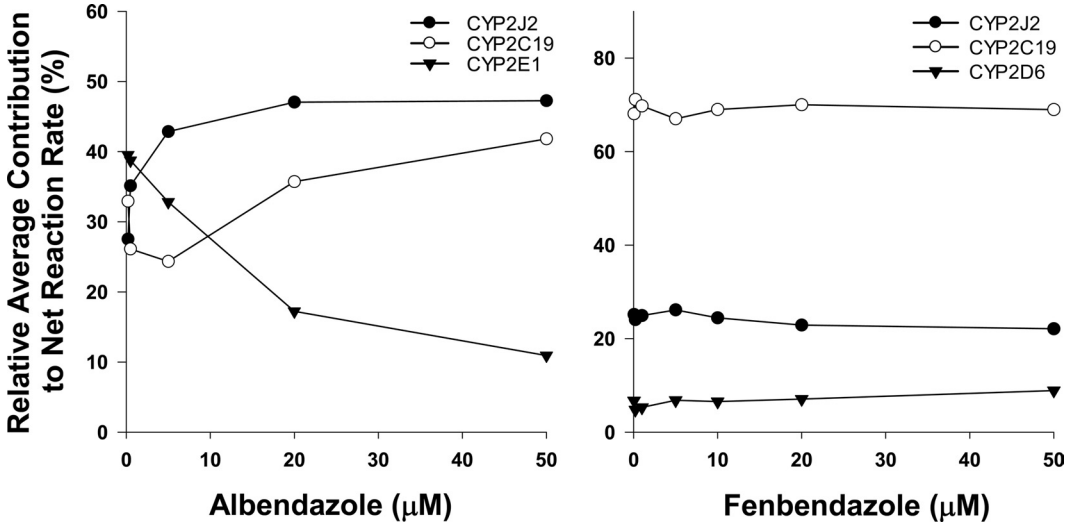

FIG 6 Abundance-adjusted simulations of the relative contributions of CYP2J2, CYP2C19, CYP2E1, and CYP2D6 to albendazole and fenbendazole hydroxylation.

(Table 2). The rates of hydroxyfenbendazole formation from fenbendazole were significantly correlated ($P < 0.05$) with the CYP2C19-mediated *S*-mephenytoin hydroxylation and CYP2J2-mediated ebastine hydroxylation activities. The significant correlation ($P = 0.02$) between fenbendazole hydroxylase activity and CYP3A activity might also be derived from the cross correlation between CYP2J2 and CYP3A activity ($P = 0.05$) in the bank of HLMs evaluated.

The kinetics of the formation of hydroxyfenbendazole from fenbendazole by rCYP2C19 and rCYP2J2 was characterized using the substrate inhibition equation (Fig. 5D and F). The Eadie-Hofstee plots of hydroxyfenbendazole formation also showed a hook in the upper region of this plot (data not shown), which is characteristic of substrate inhibition. The rate of hydroxyfenbendazole formation from fenbendazole by recombinant CYP2D6 was characterized by the Hill equation (Fig. 5E). The Eadie-Hofstee plots of hydroxyfenbendazole formation revealed concave relationships (data not shown), indicating negative ($n = 0.78$) cooperativity. The intrinsic clearance values of hydroxyfenbendazole formation by CYP2C19 (2.68 μl/min/pmol P450) and CYP2J2 (1.94 μl/min/pmol P450) were much higher than the intrinsic clearance value of hydroxyfenbendazole formation by CYP2D6 (0.23 μl/min/pmol P450) (Table 1), indicating that CYP2C19 and CYP2J2 are the major metabolizing enzymes responsible for hydroxyfenbendazole formation.

To determine the relative contributions of the three P450 isoforms to hydroxylation metabolism at different concentrations in human liver microsomes, we estimated the percentage of the net reaction rate from the abundance-adjusted simulation of each P450 isoform in human liver microsomes (Fig. 6). For this, we normalized the metabolic rates of the expressed P450 isoforms according to the abundance of the respective isoforms in the human liver, as described by Rodrigues (36) or Kim et al. (37). Briefly, the reaction rates measured with individual cDNA-expressed P450 isoforms were normalized with respect to the nominal specific content of the corresponding P450 in native human liver microsomes. In this study, we adapted the data for immunologically determined P450 isoform liver contents reported by Shimada et al. (38), Yamazaki et al. (39), Yamazaki et al. (40), and Lasker et al. (41); i.e., 2.73% for CYP2C19, 1.16% for CYP2J2, 1.5% for CYP2D6, and 6.6% for CYP2E1. In turn, the normalized rates for each cDNA-expressed P450 were summed, yielding a total normalized rate (TNR; $\sum f_i \cdot V_i$), and the normalized rate for each P450 isoform ($f_i \cdot V_i$) was expressed as a percentage of the net reaction rate $\{100 \times [(f_i \cdot V_i)/(\sum f_i \cdot V_i)]\}$, where f_i indicates the fraction of the content of each P450 isoform in the human liver, and V_i is $V_{\max,i} \cdot [S_i]/(K_{m,i} + [S_i])$, where $V_{\max}i$ is the $V_{\max}$ for each isoform, $[S_i]$ is the substrate concentration for each isoform, and $K_{m,i}$ is the K_m for each isoform. This simulation shows that CYP2C19 and CYP2J2 are the major P450 isoforms responsible for hydroxy metabolite formation from albendazole over the whole concentration range tested (0 to 50 μM). The percentage of the net reaction by CYP2E1 (about 40%) decreased rapidly with increasing albendazole concentration and reached 10% at 50 μM. CYP2C19 and CYP2J2 are the major P450 isoforms responsible for hydroxy metabolite formation from fenbendazole.

Taken together, these results suggest that CYP2J2 is one of the major enzymes involved in the hydroxylation of both albendazole and fenbendazole. CYP2J2 is expressed in the human brain, heart, kidney, liver, lung, placenta, and skeletal muscle (42) and is regarded as a minor hepatic drug-metabolizing enzyme. However, recent studies have shown CYP2J2 to be involved in the metabolism of endogenous arachidonic acid (43), as well as drugs, including amiodarone (24) astemizole (44), apixaban (45), cyclosporine (11), ebastine (25), mesoridazine (11), tamoxifen (11), and thioridazine (11). Thus, CYP2J2 could be a target of the interactions of the drugs metabolized by this enzyme. In addition, the identification of CYP2J2 as the catalyst of hydroxylation of albendazole may allow use of albendazole as a CYP2J2 probe substrate due to the nonavailability of a specific probe for measuring CYP2J2 activity *in vitro* and *in vivo*, despite identification of an increasing number of drugs for which CYP2J2 is responsible for metabolism. Our data indicate that albendazole hydroxylation is a specific *in vitro*

reaction marker of CYP2J2 and may have utility as a phenotyping tool to study the role of this enzyme in drug metabolism.

ACKNOWLEDGMENT

This work was supported by a grant from the Korea Health Technology R&D Project, Ministry of Health & Welfare, Republic of Korea (A111345).

REFERENCES

1. **Horton RJ.** 1990. Benzimidazoles in a wormy world. Parasitol. Today **6:**106.
2. **McKellar QA, Gokbulut C, Muzandu K, Benchaoui H.** 2002. Fenbendazole pharmacokinetics, metabolism, and potentiation in horses. Drug Metab. Dispos. **30:**1230–1239.
3. **Abdel-tawab, AM, Bradley M, Ghazaly EA, Horton J, el-Setouhy M.** 2009. Albendazole and its metabolites in the breast milk of lactating women following a single oral dose of albendazole. Br. J. Clin. Pharmacol. **68:**737–742.
4. **Virkel G, Lifschitz A, Sallovitz J, Pis A, Lanusse C.** 2004. Comparative hepatic and extrahepatic enantioselective sulfoxidation of albendazole and fenbendazole in sheep and cattle. Drug Metab. Dispos. **32:**536–544.
5. **Murray M, Hudson AM, Yassa V.** 1992. Hepatic microsomal metabolism of the anthelmintic benzimidazole fenbendazole: enhanced inhibition of cytochrome P450 reactions by oxidized metabolites of the drug. Chem. Res. Toxicol. **5:**60–66.
6. **Montesissa C, Stracciari JM, Fadini L, Beretta C.** 1989. Comparative microsomal oxidation of febantel and its metabolite fenbendazole in various animal species. Xenobiotica **19:**97–100.
7. **Gottschall DW, Theodorides VJ, Wang R.** 1990. The metabolism of benzimidazole anthelmintics. Parasitol. Today **6:**115–124.
8. **Lanusse CE, Prichard RK.** 1993. Clinical pharmacokinetics and metabolism of benzimidazole anthelmintics in ruminants. Drug Metab. Rev. **25:**235–279.
9. **Rawden HC, Kokwaro GO, Ward SA, Edwards G.** 2000. Relative contribution of cytochromes P-450 and flavin-containing monoxygenases to the metabolism of albendazole by human liver microsomes. Br. J. Clin. Pharmacol. **49:**313–322.
10. **Souhaili-El Amri H, Mothe O, Totis M, Masson C, Batt AM, Delatour P, Siest G.** 1988. Albendazole sulfonation by rat liver cytochrome P-450c. J. Pharmacol. Exp. Ther. **246:**758–764.
11. **Lee CA, Neul D, Clouser-Roche A, Dalvie D, Wester MR, Jiang Y, Jones JP, III, Freiwald S, Zientek M, Totah RA.** 2010. Identification of novel substrates for human cytochrome P450 2J2. Drug Metab. Dispos. **38:**347–356.
12. **Short CR, Barker SA, Hsieh LC, Ou SP, McDowell T, Davis LE, Neff-Davis CA, Koritz G, Bevill RF, Munsiff IJ.** 1987. Disposition of fenbendazole in cattle. Am. J. Vet. Res. **48:**958–961.
13. **Garcia HH, Evans CA, Nash TE, Takayanagui OM, White AC, Jr, Botero D, Rajshekhar V, Tsang VC, Schantz PM, Allan JC, Flisser A, Correa D, Sarti E, Friedland JS, Martinez SM, Gonzalez AE, Gilman RH, Del Brutto OH.** 2002. Current consensus guidelines for treatment of neurocysticercosis. Clin. Microbiol. Rev. **15:**747–756.
14. **Garcia HH, Lescano AG, Lanchote VL, Pretell EJ, Gonzales I, Bustos JA, Takayanagui OM, Bonato PS, Horton J, Saavedra H, Gonzalez AE, Gilman RH, Cysticercosis Working Group in Peru.** 2011. Pharmacokinetics of combined treatment with praziquantel and albendazole in neurocysticercosis. Br. J. Clin. Pharmacol. **72:**77–84.
15. **Marriner SE, Morris DL, Dickson B, Bogan JA.** 1986. Pharmacokinetics of albendazole in man. Eur. J. Clin. Pharmacol. **30:**705–708.
16. **Mpairwe H, Webb EL, Muhangi L, Ndibazza J, Akishule D, Nampijja M, Ngom-wegi S, Tumusime J, Jones FM, Fitzsimmons C, Dunne DW, Muwanga M, Rodrigues LC, Elliott AM.** 2011. Anthelminthic treatment during pregnancy is associated with increased risk of infantile eczema: randomised-controlled trial results. Pediatr. Allergy Immunol. **22:**305–312.
17. **Elliott AM, Ndibazza J, Mpairwe H, Muhangi L, Webb EL, Kizito D, Mawa P, Tweyongyere R, Muwanga M, Entebbe Mother and Baby Study Team.** 2011. Treatment with anthelminthics during pregnancy: what gains and what risks for the mother and child? Parasitology **138:**1499–1507.
18. **Cortes EC, Mendoza RS, Gutierrez MS, de Cortes OGM.** 2004. Efficient synthesis in three steps and spectral determination of methyl-5-[(o-, m-, and p-substituted-phenylthio]-2-benzimidazolecarbamates. J. Heterocyclic Chem. **41:**273–276.
19. **Lee T, Lee D, Lee IY, Gong YD.** 2010. Solid-phase synthesis of thiazolo[4,5-b]pyridine derivatives using Friedlander reaction. J. Combinatorial Chem. **12:**95–99.
20. **Lee T, Park JH, Lee DH, Gong YD.** 2009. Traceless solid-phase synthesis of 2,4,6-trisubstituted thiazolo[4,5-d]pyrimidine-5,7-dione derivatives. J. Combinatorial Chem. **11:**495–499.
21. **Lee T, Park JH, Jeon MK, Gong YD.** 2009. Solid-phase synthesis of 1,3,6-trisubstituted-1H-thiazolo[4,5-c][1,2]thiazin-4(3H)one-2,2-dioxide derivatives using traceless linker. J. Combinatorial Chem. **11:**288–293.
22. **Kim MJ, Kim H, Cha IJ, Park JS, Shon JH, Liu KH, Shin JG.** 2005. High-throughput screening of inhibitory potential of nine cytochrome P450 enzymes in vitro using liquid chromatography/tandem mass spectrometry. Rapid Commun. Mass Spectrom. **19:**2651–2658.
23. **Ha-Duong NT, Dijols S, Macherey AC, Goldstein JA, Dansette PM, Mansuy D.** 2001. Ticlopidine as a selective mechanism-based inhibitor of human cytochrome P450 2C19. Biochemistry **40:**12112–12122.
24. **Lee CA, Jones JP, III, Katayama J, Kaspera R, Jiang Y, Freiwald S, Smith E, Walker GS, Totah RA.** 2012. Identifying a selective substrate and inhibitor pair for the evaluation of CYP2J2 activity. Drug Metab. Dispos. **40:**943–951.
25. **Liu KH, Kim MG, Lee DJ, Yoon YJ, Kim MJ, Shon JH, Choi CS, Choi YK, Desta Z, Shin JG.** 2006. Characterization of ebastine, hydroxyebastine, and carebastine metabolism by human liver microsomes and expressed cytochrome P450 enzymes: major roles for CYP2J2 and CYP3A. Drug Metab. Dispos. **34:**1793–1797.
26. **Yoon YJ, Liu KH.** 2011. Potential of hydroxyebastine and terfenadine alcohol to inhibit the human cytochrome P450 2J2 isoform. J. Korean Soc. Appl. Biol. **54:**659–666.
27. **Liu K.** 2011. Screening of potential anticancer compounds from marketed drugs: aripiprazole, haloperidol, miconazole, and terfenadine inhibit cytochrome P450 2J2. Korean J. Life Sci. **21:**1558–1564.
28. **Yoon YJ, Kim KB, Kim H, Seo KA, Kim HS, Cha IJ, Kim EY, Liu KH, Shin JG.** 2007. Characterization of benidipine and its enantiomers' metabolism by human liver cytochrome p450 enzymes. Drug Metab. Dispos. **35:**1518–1524.
29. **Heyn H, White RB, Stevens JC.** 1996. Catalytic role of cytochrome P4502B6 in the N-demethylation of S-mephenytoin. Drug Metab. Dispos. **24:**948–954.
30. **Li W, Liu Y, He YQ, Zhang JW, Gao Y, Ge GB, Liu HX, Huo H, Liu HT, Wang LM, Sun J, Wang Q, Yang L.** 2008. Characterization of triptolide hydroxylation by cytochrome P450 in human and rat liver microsomes. Xenobiotica **38:**1551–1565.
31. **Ghosal A, Ramanathan R, Yuan Y, Hapangama N, Chowdhury SK, Kishnani NS, Alton KB.** 2007. Identification of human liver cytochrome P450 enzymes involved in biotransformation of vicriviroc, a CCR5 receptor antagonist. Drug Metab. Dispos. **35:**2186–2195.
32. **Luo JP, Vashishtha SC, Hawes EM, McKay G, Midha KK, Fang J.** 2011. In vitro identification of the human cytochrome p450 enzymes involved in the oxidative metabolism of loxapine. Biopharm. Drug Dispos. **32:**398–407.
33. **Kim KH, Kim DH, Jang HH, Kim M, Kim DH, Kim JS, Kim JI, Chae HZ, Ahn T, Yun CH.** 2007. Lateral segregation of anionic phospholipids in model membranes induced by cytochrome P450 2B1: bi-directional coupling between CYP2B1 and anionic phospholipid. Arch. Biochem. Biophys. **468:**226–233.
34. **Collom SL, Laddusaw RM, Burch AM, Kuzmic P, Perry MD, Jr, Miller GP.** 2008. CYP2E1 substrate inhibition. Mechanistic interpretation through an effector site for monocyclic compounds. J. Biol. Chem. **283:**3487–3496.
35. **Dayan AD.** 2003. Albendazole, mebendazole and praziquantel. Review of non-clinical toxicity and pharmacokinetics. Acta Trop. **86:**141–159.
36. **Rodrigues AD.** 1999. Integrated cytochrome P450 reaction phenotyping: attempting to bridge the gap between cDNA-expressed cytochromes P450 and native human liver microsomes. Biochem. Pharmacol. **57:**465–480.
37. **Kim KA, Kim MJ, Park JY, Shon JH, Yoon YR, Lee SS, Liu KH, Chun JH, Hyun MH, Shin JG.** 2003. Stereoselective metabolism of lansoprazole by human liver cytochrome P450 enzymes. Drug Metab. Dispos. **31:**1227–1234.
38. **Shimada T, Yamazaki H, Mimura M, Inui Y, Guengerich FP.** 1994.

Interindividual variations in human liver cytochrome P-450 enzymes involved in the oxidation of drugs, carcinogens and toxic chemicals: studies with liver microsomes of 30 Japanese and 30 Caucasians. J. Pharmacol. Exp. Ther. **270:**414–423.

39. **Yamazaki H, Inoue K, Shaw PM, Checovich WJ, Guengerich FP, Shimada T.** 1997. Different contributions of cytochrome P450 2C19 and 3A4 in the oxidation of omeprazole by human liver microsomes: effects of contents of these two forms in individual human samples. J. Pharmacol. Exp. Ther. **283:**434–442.
40. **Yamazaki H, Okayama A, Imai N, Guengerich FP, Shimizu M.** 2006. Inter-individual variation of cytochrome P4502J2 expression and catalytic activities in liver microsomes from Japanese and Caucasian populations. Xenobiotica **36:**1201–1209.
41. **Lasker JM, Wester MR, Aramsombatdee E, Raucy JL.** 1998. Characterization of CYP2C19 and CYP2C9 from human liver: respective roles in microsomal tolbutamide, S-mephenytoin, and omeprazole hydroxylations. Arch. Biochem. Biophys. **353:**16–28.
42. **Zeldin DC, Foley J, Ma J, Boyle JE, Pascual JM, Moomaw CR, Tomer KB, Steenbergen C, Wu S.** 1996. CYP2J subfamily P450s in the lung: expression, localization, and potential functional significance. Mol. Pharmacol. **50:**1111–1117.
43. **Spiecker M, Darius H, Hankeln T, Soufi M, Sattler AM, Schaefer JR, Node K, Borgel J, Mugge A, Lindpaintner K, Huesing A, Maisch B, Zeldin DC, Liao JK.** 2004. Risk of coronary artery disease associated with polymorphism of the cytochrome P450 epoxygenase CYP2J2. Circulation **110:**2132–2136.
44. **Matsumoto S, Yamazoe Y.** 2001. Involvement of multiple human cytochromes P450 in the liver microsomal metabolism of astemizole and a comparison with terfenadine. Br. J. Clin. Pharmacol. **51:**133–142.
45. **Wang L, Zhang D, Raghavan N, Yao M, Ma L, Frost CE, Maxwell BD, Chen SY, He K, Goosen TC, Humphreys WG, Grossman SJ.** 2010. In vitro assessment of metabolic drug-drug interaction potential of apixaban through cytochrome P450 phenotyping, inhibition, and induction studies. Drug Metab. Dispos. **38:**448–458.